Chemical Science

ROYAL SOCIETY OF CHEMISTRY

EDGE ARTICLE

View Article Online
View Journal | View Issue



Check for updates

Cite this: *Chem. Sci.*, 2023, **14**, 3363

All publication charges for this article have been paid for by the Royal Society of Chemistry

Received 1st December 2022
Accepted 27th February 2023

DOI: 10.1039/d2sc06621a

rsc.li/chemical-science

# Chemical energy assisted self-assembling of a porphyrin-substituted benzoic acid in complex environments†

Bingxu Ma, Bowen Pang, Wang Zeng,* Huimin Fu, Yi Jiang, Shenglin Yao, Yida Yang, Kaisheng Zhu and Wei Zhang *

Energy input plays a crucial role in the assembling of matter. In our present study, we utilize **EDC** as a chemical fuel to drive the molecular assembling of **POR-COOH**. **POR-COOH** will react with **EDC** to generate the intermediate **POR-COOEDC** first, which was well-solvated by solvent molecules. During the subsequent hydrolysis process, **EDU** and oversaturated **POR-COOH** molecules at high energy states will be formed and thus allowed the self-assembling of **POR-COOH** into 2D nanosheets. This chemical energy assisted assembling process could be performed not only under mild conditions with high spatial accuracy but also with high selectivity in complex environments.

## Introduction

During the transition of matter from one state to another through assembling, energy input is crucial for activating molecules to overcome the energy barrier during the process (Fig. 1). In general, importing energy into the system and promoting molecules to the required energy level for assembling could be achieved in multiple ways, such as heating, solvation with a good solvent, irradiation with light, excitation under external fields, tuning the pH value, or a combination of them.[1]

In a chemical reaction, the energy will exchange and redistribute among reactants, products and intermediates (if there are any) constantly, thus affording the possibility for the molecules involved in the reaction to assemble. Representative examples have been reported as 'reaction-triggered self-assemblings' in the past few decades.[2] During these processes, despite the starting matter being consumed and converted into different chemical species, the as-formed products were able to assemble and form ordered supramolecular structures. Here we report that using the energy released during a chemical reaction cycle, we are able to drive molecules to self-assemble and form highly ordered supramolecular structures without changing the chemical structure of molecules at the final stage. More importantly, this chemical energy assisted assembling process could be performed under mild conditions with high spatial accuracy and selectivity.

## Results and discussion

We found this chemical energy assisted self-assembling process during the study of the reaction between carbodiimide and carboxylic acid derivates. It is well known that during the reaction between carboxylic acid and carbodiimide (such as 1-ethyl-3-(3-dimethylaminopropyl)carbodiimide, **EDC**), the corresponding anhydride will be generated as an intermediate first, and then hydrolyze into the original carboxylic acid in the presence of water (Fig. 2a).[3] With the continuously supported compound **EDC** as the chemical fuel, these anhydrides were able to further assemble into functional transient supramolecular structures, as demonstrated by Boekhoven, Hartley and other groups.[3b,4] However, in our present study, we noticed that the reaction between **EDC** and a porphyrin-substituted benzoic acid (**POR-**

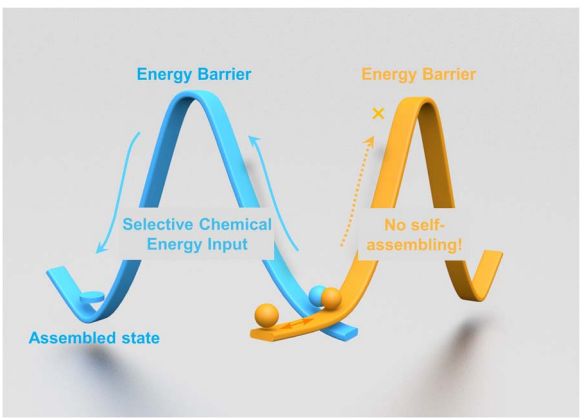


Fig. 1 Schematic representation of the chemical energy assisted self-assembling.

*South China Advanced Institute for Soft Matter Science and Technology, School of Emergent Soft Matter and Guangdong Provincial Key Laboratory of Functional and Intelligent Hybrid Materials and Devices, South China University of Technology, Guangzhou 510640, China. E-mail: zengwang@scut.edu.cn; weizhang@scut.edu.cn*

† Electronic supplementary information (ESI) available. See DOI: https://doi.org/10.1039/d2sc06621a

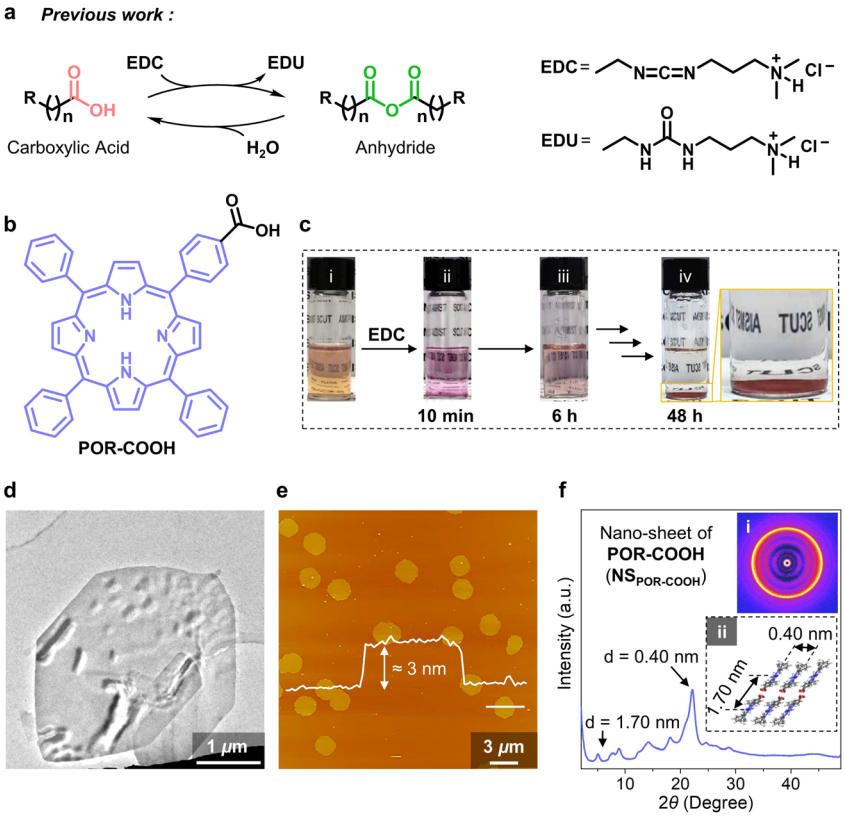


Fig. 2 (a) Formation of a transient anhydride intermediate from carboxylic acid derivates driven by **EDC**. (b) Molecular structure of **POR-COOH**. (c) Photographs of the reaction mixture of the **POR-COOH** suspension and **EDC** at different moments. (d) TEM micrograph of an air-dried dispersion of $\mathbf{NS}_{\mathbf{POR\text{-}COOH}}$. (e) Liquid phase AFM micrograph of $\mathbf{NS}_{\mathbf{POR\text{-}COOH}}$ in the presence of solvent. (f) WAXD profile of $\mathbf{NS}_{\mathbf{POR\text{-}COOH}}$ and its 2D WAXD pattern (inset i) and proposed packing model (inset ii).

**COOH**, Fig. 2b) did not result in the insoluble anhydride intermediate. For instance, we started from a suspension of amorphously aggregated **POR-COOH** ($\mathbf{AA}_{\mathbf{POR\text{-}COOH}}$, 0.066 mg, $1.0 \times 10^{-4}$ mmol **POR-COOH** in 2.0 mL DMSO–$H_2O$ (6/4, v/v), Fig. S1 and S2†). When 1.2 mg **EDC** ($6.0 \times 10^{-3}$ mmol, 60 equiv.) was added into the system, we first found that the brown suspension (Fig. 2c(i)) turned to a transparent pink solution within 10 minutes (Fig. 2c(ii)), and then gradually turned into a turbid suspension (Fig. 2c(iii)) and eventually yielded a red precipitate after 48 h (Fig. 2c(iv)).

After completely dissolving the red precipitate in DMSO-$d_6$, we found that its $^1$H NMR spectrum was identical to that of compound **POR-COOH** (Fig. S3†), which suggested that the red precipitate has an identical chemical composition to starting **POR-COOH**. In the meantime, the transmission electron microscopy (TEM) images of an air-dried sample allowed for the visualization of nano-sheets with side lengths up to micrometers (Fig. 2d). From scanning electron microscopy (SEM), we found that these nano-sheets stacked together on the substrate during solvent evaporation (Fig. S4†). Fortunately, liquid-phase atomic force microscopy (AFM) allowed us to conduct the measurement without removing the solvent and provided us the opportunity to observe the morphology of the resulting assemblies *in situ*. As shown in Fig. 2e, the AFM micrograph clearly proved the formation of two-dimensional (2D) nano-sheets with a uniform thickness of 3.0 nm. Considering the reported packing model of porphyrin derivatives,[5] we presume that the 2D nano-sheets of **POR-COOH** ($\mathbf{NS}_{\mathbf{POR\text{-}COOH}}$) are constructed from *J*-aggregated **POR-COOH** molecules (Fig. 2f and S5†), and the simulated wide-angle X-ray diffraction (WAXD) profile of this proposed stacking model is consistent with the experimental measurement (Fig. S6†). These results indicate that the resulting red precipitate is compound **POR-COOH** in the form of $\mathbf{NS}_{\mathbf{POR\text{-}COOH}}$ with a high degree of crystallinity.

Utilizing ultraviolet-visible (UV-vis) absorption and dynamic light scattering (DLS) spectroscopy, we are able to monitor the entire process. The UV-vis absorption spectrum of $\mathbf{AA}_{\mathbf{POR\text{-}COOH}}$ suspension ($0.50 \times 10^{-4}$ M in DMSO–$H_2O$ (6/4, v/v)) showed a maximum absorption peak at 417 nm along with a shoulder peak at 437 nm (Fig. 3a, green curve), characteristic of the *J*-aggregated **POR-COOH**.[6] After adding **EDC** (60 equiv.) into the $\mathbf{AA}_{\mathbf{POR\text{-}COOH}}$ suspension, the shoulder peak at 437 nm disappeared, while the intensity of the peak at 417 nm increased within 10 minutes (Fig. 3a), which suggested that the aggregated **POR-COOH** was converted into a solvated intermediate.[6c] After 10 minutes, the peak at 417 nm gradually decreased, with the intensity increase of the shoulder peak at 437 nm, indicating that the solvated intermediate turned into *J*-aggregated **POR-COOH** again (Fig. 3b). When we plot the absorption intensity at 417 nm *versus* time, a maximum absorption was found at 10 minutes

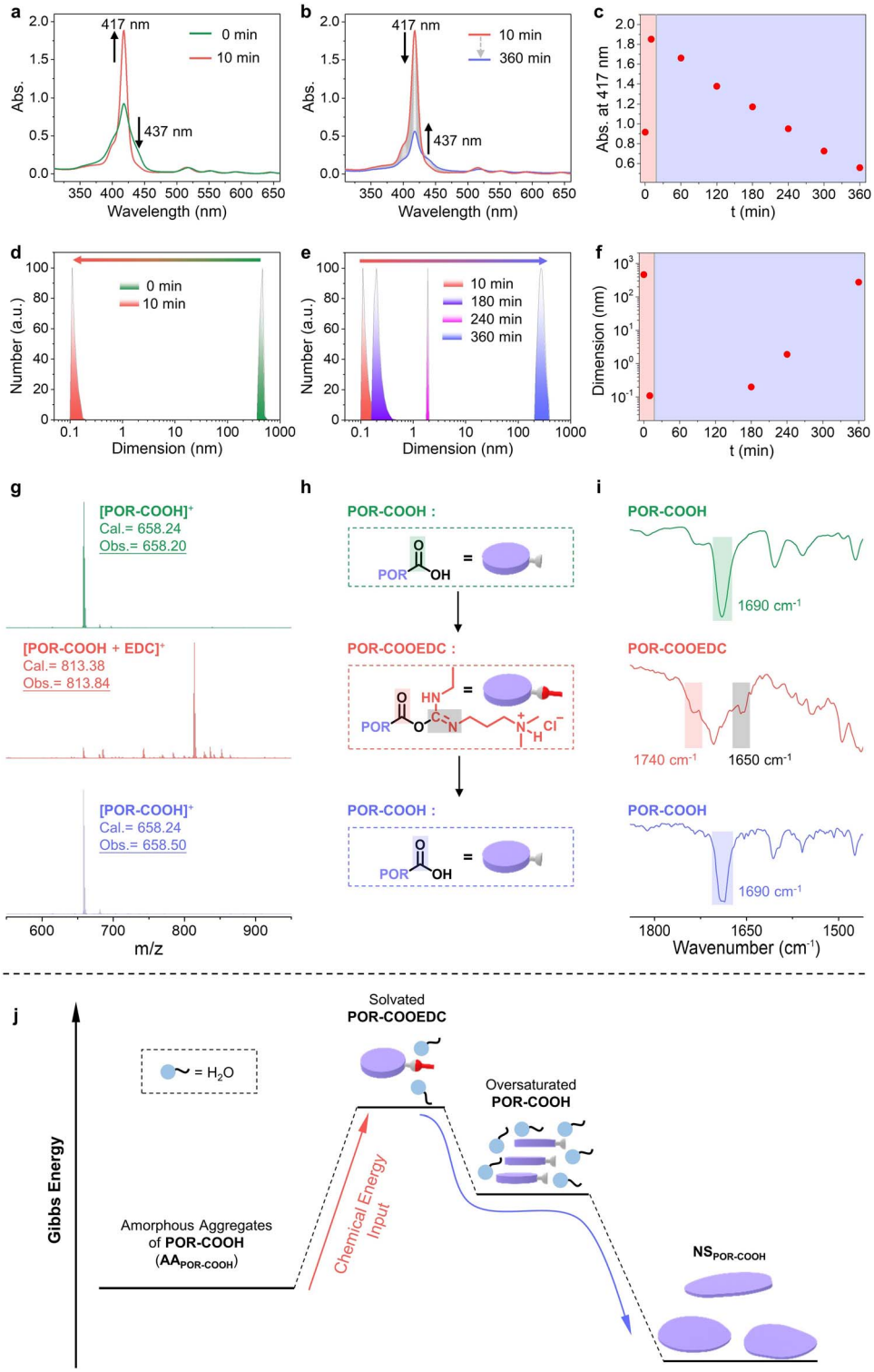


Fig. 3 (a and b) Time-dependent absorption spectra of $AA_{POR\text{-}COOH}$ after the addition of **EDC**. (c) Time-dependent absorption intensity at 417 nm. (d and e) Time-dependent size distribution of $AA_{POR\text{-}COOH}$ monitored by DLS after the addition of **EDC**. (f) Plot of the particle size *versus* time, monitored by DLS. (g) MALDI-TOF mass spectra of $AA_{POR\text{-}COOH}$ (green curve), $AA_{POR\text{-}COOH}$ reacts with **EDC** for several minutes (red curve), and $NS_{POR\text{-}COOH}$ (blue curve). (h) Schematic representation of the reaction cycle between **POR-COOH** and **EDC**. (i) FT-IR spectra of $AA_{POR\text{-}COOH}$ (green curve), **POR-COOEDC** (red curve), and $NS_{POR\text{-}COOH}$ (blue curve). (j) Schematic illustration of the mechanism of the chemical energy assisted self-assembling process in this study.

after adding **EDC** (Fig. 3c). From the DLS profiles, we found objects with sizes up to several hundreds of nanometers in the $\mathbf{AA_{POR\text{-}COOH}}$ suspension, and they decrease to less than 1 nanometer in 10 minutes after adding **EDC** (Fig. 3d), followed by gradually increasing to several hundreds of nanometers again in 360 minutes (Fig. 3e). The observed time-dependent size variation pattern (Fig. 3f) matched with time-dependent absorption spectra very well. Later we are able to identify the intermediate utilizing matrix-assisted laser desorption ionization time-of-flight (MALDI-TOF) mass and Fourier transform infrared (FT-IR) spectroscopy. As expected, the MALDI-TOF mass spectra of $\mathbf{AA_{POR\text{-}COOH}}$ and $\mathbf{NS_{POR\text{-}COOH}}$ displayed a major peak at $m/z$ = 658.20 and 658.50, respectively (Fig. 3g, green and blue curves), which matched with the molecular weight of **POR-COOH** (calcd $m/z$ = 658.24), since they have identical chemical composition. However, the MALDI-TOF mass spectrum of the soluble intermediate showed the presence of a fraction with a different molecular weight at $m/z$ = 813.38 (Fig. 3g, red curve), and no other chemical composition, such as anhydride, was detected. This value ($m/z$ = 813.38) equals the sum of the molecular weight of **POR-COOH** and **EDC**. Considering the reported reaction mechanism between **EDC** and carboxylic acid derivatives,[3b,7] we suspected that an **EDC**-ester **POR-COOEDC** was formed as an intermediate first, and then hydrolyzed into **POR-COOH**, due to its high chemical activity (Fig. 3h). To examine our assumption, we used FT-IR spectroscopy to trace the reaction process. We found that $\mathbf{AA_{POR\text{-}COOH}}$ and $\mathbf{NS_{POR\text{-}COOH}}$ showed almost identical IR spectra, with the stretch vibration peak of the C=O bond in

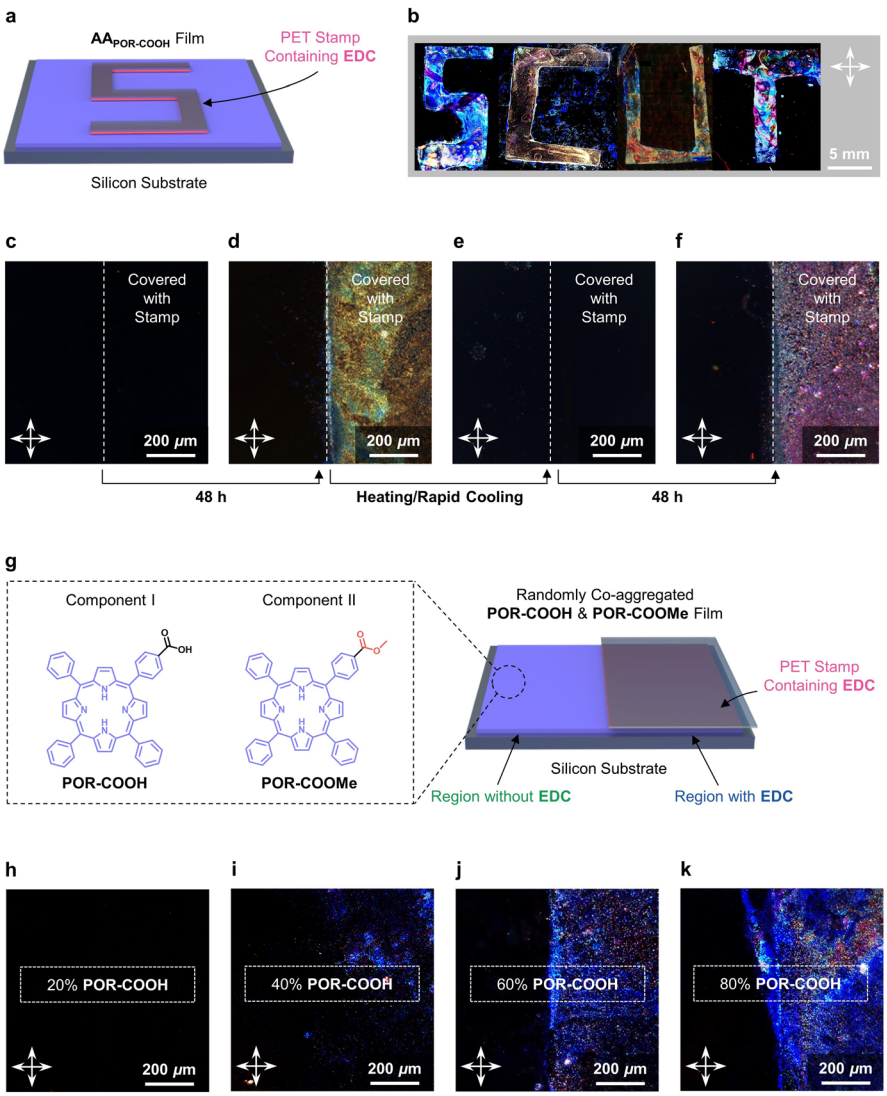


Fig. 4 (a) The schematic illustration of the experimental setup for spatial controlled chemical energy-assisted assembling of the $\mathbf{AA_{POR\text{-}COOH}}$ film. (b) Polarized light microscopy images of the $\mathbf{AA_{POR\text{-}COOH}}$ film covered by PET stamps shaped into "SCUT" letters. (c–f) Polarized light microscopy images of (c) the $\mathbf{AA_{POR\text{-}COOH}}$ film, (d) covered with the PET stamp on the right side for 48 h, (e) erasing the alignment of molecules by heating and rapid cooling, and (f) covered with the PET stamp on the right side for 48 h again. (g) Experimental setup of the chemical energy assisted self-assembling process for the spin-coated $\mathbf{AA_{POR\text{-}COOH\&POR\text{-}COOMe}}$ film. (h–k) Polarized light microscopy images of $\mathbf{AA_{POR\text{-}COOH\&POR\text{-}COOMe}}$ films covered with the PET stamp containing **EDC** for 48 h. Molar contents of **POR-COOH** in the mixture were (h) 20%, (i) 40%, (j) 60%, and (k) 80%, respectively. The white crossed arrows indicate the direction of the polarizer and the analyzer.

the carboxylic group at 1690 $cm^{-1}$ (Fig. 3i, green and blue curves). However, after adding **EDC**, the intermediate separated from the pink solution displayed two new peaks at 1740 $cm^{-1}$ and 1650 $cm^{-1}$ (Fig. 3i, red curve), which could be assigned to the C=O bond in ester groups and the C=N bond on the side chain, respectively.[7a,8] Alternatively, using water-free conditions, we are able to isolate this intermediate **POR-COOEDC** and identified its chemical structure by $^1H$ NMR spectroscopy (Fig. S7†) clearly.

Taking into account all above results, we are able to conclude the mechanism of this chemical energy assisted assembling process (Fig. 3j). The starting material **POR-COOH** has low solubility in certain solvents, such as DMSO–$H_2O$ (6/4, v/v). Without a proper self-assembling process, **POR-COOH** tends to aggregate randomly and forms an amorphous aggregated structure (Fig. S1†). Once **EDC** was added into the system, **POR-COOH** will be converted into intermediate product **POR-COOEDC** at the early stage of the reaction. **POR-COOEDC** has higher solubility and will be solvated by water molecules and form a pink transparent solution. Later, when **POR-COOH** was re-generated from the hydrolysis of solvated **POR-COOEDC**, the insoluble **POR-COOH** molecules were still surrounded by solvent molecules temporarily and thus existed as an over-saturated high energy state, which allowed them to self-assemble into 2D nano-sheets. In this reaction cycle, the net reaction is the high-energy chemical species **EDC** was converted into the low-energy chemical species **EDU**, and in the meantime, the chemical energy released during the reaction was transferred to $\mathbf{AA_{POR\text{-}COOH}}$ and promoted **POR-COOH** molecules to a high energy state, followed by self-assembling into 2D nano-sheets.

This chemical energy assisted self-assembling process could be performed under conditions close to solvent-free environments. As shown in Fig. S8†, a thin film of $\mathbf{AA_{POR\text{-}COOH}}$ (see the ESI† for fabrication details) shows no birefringence in polarized light microscopy (POM) under crossed polarizers, due to the random alignment of **POR-COOH** molecules. In contrast, the assembled crystalline $\mathbf{NS_{POR\text{-}COOH}}$ shows birefringence due to the highly ordered molecular alignment in the 2D nano-sheet assembly (Fig. S9†). When a thin film composed of $\mathbf{AA_{POR\text{-}COOH}}$ was covered by PET stamps (shaped to letters "S", "C", "U", and "T") soaked with the **EDC** solution (0.1 M in DMSO–$H_2O$ (6/4, v/v)) for 48 h (Fig. 4a), a bright "SCUT" pattern was observed under the crossed polarizers, after removing the chemical energy stamps (Fig. 4b). That means that amorphously aggregated $\mathbf{AA_{POR\text{-}COOH}}$ located in the area covered by PET stamps were assembled into $\mathbf{NS_{POR\text{-}COOH}}$ with high spatial accuracy. We further confirmed that this chemical energy-assisted assembling process could be repeated many times. Starting from a thin film of $\mathbf{AA_{POR\text{-}COOH}}$ as shown in Fig. 4c, we could first promote the molecules on the right side to self-assemble by using a PET stamp soaked with **EDC** solution (Fig. 4d), erasing the alignment of molecules to amorphous states by heating and rapid cooling (Fig. 4e), and then drive them to assemble into $\mathbf{NS_{POR\text{-}COOH}}$ by using the PET stamp again (Fig. 4f).

Due to the selectivity of chemical reactions, our chemical energy assisted assembling process could also be performed selectively under complex environments, such as in the presence of porphyrin derivatives with a similar chemical structure (**POR-COOMe**, Fig. 4g). To demonstrate it, we prepared thin films composed of amorphous aggregates of a mixture of **POR-COOH** and **POR-COOMe** ($\mathbf{AA_{POR\text{-}COOH\&POR\text{-}COOMe}}$, the molar contents of **POR-COOH** in the mixture were 20%, 40%, 60%, and 80%, respectively) on silicon substrates accordingly (see the ESI† for fabrication details). After covering the right side of these thin films with PET stamps soaked with **EDC** solution for 48 h, birefringence was detected on the area covered by **EDC**. More importantly, we found that the intensity of the birefringence was amplified with the increasing amount of **POR-COOH** in the mixture (Fig. 4h–k). These observations clearly suggested that, despite the structural similarity between **POR-COOH** and **POR-COOMe**, only compound **POR-COOH** was activated by the energy released during this chemical reaction cycle, and assembled into nano-sheets.

Finally, taking advantage of the high selectivity and spatial accuracy of this chemical energy assisted assembling process, we are able to transfer energy to **POR-COOH** molecules in a mixture selectively and drive **POR-COOH** molecules to self-assemble in a separated domain. The experiment was carried out on a hydrogel with an inert polyacrylamide framework

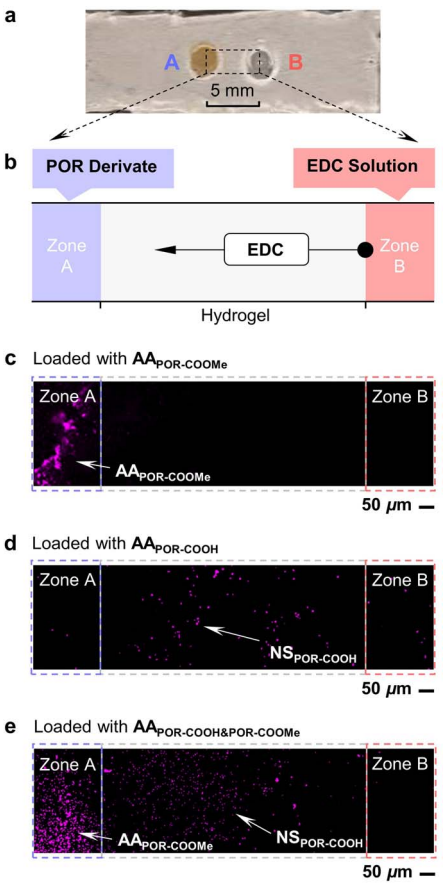


Fig. 5 (a) Experimental setup for chemical energy assisted assembling in a hydrogel with inert frameworks. (b) Schematic drawing of the experimental setup. (c–e) CLSM micrographs of samples when (c) $AA_{POR\text{-}COOMe}$, (d) $AA_{POR\text{-}COOH}$, and (e) $AA_{POR\text{-}COOH\&POR\text{-}COOMe}$ were loaded in zone A, respectively.

(Fig. 5a), with the ability to prevent the Brownian motion of the aggregated objects. As shown in Fig. 5b, zone B was always filled with **EDC** solution (50 mM in 3.0 μL DMSO–$H_2O$ (6/4, v/v)). When zone A was loaded with $\mathbf{AA_{POR\text{-}COOMe}}$ suspension (0.50 mM in 5.0 μL DMSO–$H_2O$ (6/4, v/v)), we found that all **POR-COOMe** still remained in zone A after 48 h (Fig. 5c), since $\mathbf{AA_{POR\text{-}COOMe}}$ was too large to move inside the inert hydrogel framework. In contrast, when zone A was loaded with $\mathbf{AA_{POR\text{-}COOH}}$ suspension (0.50 mM in 5.0 μL DMSO–$H_2O$ (6/4, v/v)) instead, we found that almost all **POR-COOH** was moved out from zone A and distributed in the region in-between zones A and B (Fig. 5d), possibly due to the diffusion of the soluble intermediate **POR-COOEDC**. When amorphous aggregates composed of a **POR-COOH** (0.50 mM) and **POR-COOMe** (0.50 mM) mixture were used in zone A, after 24 h, we found that the starting mixture of porphyrin derivatives was separated into two fractions in different domains (Fig. 5e). Combining the results from Fig. 5, we could conclude that the compound **POR-COOMe** from the mixture remained in zone A (possibly in an amorphously aggregated states), while compound **POR-COOH** self-assembled into $\mathbf{NS_{POR\text{-}COOH}}$ in the presence of **EDC** fuel and re-located to the region in-between zones A and B. In another word, in the presence of the **EDC** gradient, despite the structural similarity between **POR-COOH** and **POR-COOMe**, **POR-COOH** molecules were selectively driven into a separated domain during the chemical energy assisted assembling process.

## Conclusions

In conclusion, we have successfully demonstrated that the energy released during the hydrolysis of **EDC** to **EDU** could be utilized to selectively drive a porphyrin-substituted benzoic acid to self-assemble into highly ordered supramolecular structures. Considering that this chemical energy assisted assembling process could be performed not only under mild conditions with high spatial accuracy but also with high selectivity in complex environments, we believe that our strategy will provide a big innovation in both nanofabrication and supramolecular chemistry.

## Author contributions

The manuscript was written through contributions of all authors. All authors have given approval to the final version of the manuscript.

## Conflicts of interest

There are no conflicts to declare.

## Acknowledgements

This work is supported by the Guangdong Natural Science Foundation (No. 2018B030306039), Science and Technology Projects in Guangzhou (No. 202201010557), China Postdoctoral Science Foundation (No. 2021M701237), 111 Project (No. B18023) and Recruitment Program of Guangdong (No. 2016ZT06C322).

## References

1 (*a*) D. Philp and J. F. Stoddart, *Angew. Chem., Int. Ed.*, 1996, **35**, 1154; (*b*) G. M. Whitesides and B. Grzybowski, *Science*, 2002, **295**, 2418; (*c*) T. F. A. De Greef, M. M. J. Smulders, M. Wolffs, A. P. H. J. Schenning, R. P. Sijbesma and E. W. Meijer, *Chem. Rev.*, 2009, **109**, 5687; (*d*) C. Rest, R. Kandanelli and G. Fernández, *Chem. Soc. Rev.*, 2015, **44**, 2543.

2 (*a*) W. Jin, T. Fukushima, A. Kosaka, M. Niki, N. Ishii and T. Aida, *J. Am. Chem. Soc.*, 2005, **127**, 8284; (*b*) W. Wan and C. Pan, *Macromolecules*, 2007, **40**, 8897; (*c*) W. Ji, J. Yan, E. Chen, Z. Li and D. Liang, *Macromolecules*, 2008, **41**, 4914; (*d*) C. Trinh, M. T. Whited, A. Steiner, C. J. Tassone, M. F. Toney and M. E. Thompson, *Chem. Mater.*, 2012, **24**, 2583; (*e*) J. Boekhoven, J. M. Poolman, C. Maity, F. Li, L. van der Mee, C. B. Minkenberg, E. Mendes, J. H. van Esch and R. Eelkema, *Nat. Chem.*, 2013, **5**, 433; (*f*) H. Xia, H. Fu, Y. Zhang, K. C. Shih, Y. Ren, M. Anuganti, M. P. Nieh, J. Cheng and Y. Lin, *J. Am. Chem. Soc.*, 2017, **139**, 11106; (*g*) S. Panja, A. M. Fuentes-Caparrós, E. R. Cross, L. Cavalcanti and D. J. Adams, *Chem. Mater.*, 2020, **32**, 5264; (*h*) J. Park, J.-M. Heo, S. Seong, J. Noh and J.-M. Kim, *Nat. Commun.*, 2021, **12**, 4207.

3 (*a*) L. S. Kariyawasam and C. S. Hartley, *J. Am. Chem. Soc.*, 2017, **139**, 11949; (*b*) M. Tena-Solsona, B. Rieß, R. K. Grötsch, F. C. Löhrer, C. Wanzke, B. Käsdorf, A. R. Bausch, P. Müller-Buschbaum, O. Lieleg and J. Boekhoven, *Nat. Commun.*, 2017, **8**, 15895.

4 (*a*) M. M. Hossain, J. L. Atkinson and C. S. Hartley, *Angew. Chem., Int. Ed.*, 2020, **59**, 13807; (*b*) P. S. Schwarz, L. Tebcharani, J. E. Heger, P. Müller-Buschbaum and J. Boekhoven, *Chem. Sci.*, 2021, **12**, 9969; (*c*) P. S. Schwarz, S. Laha, J. Janssen, T. Huss, J. Boekhoven and C. A. Weber, *Chem. Sci.*, 2021, **12**, 7554; (*d*) F. Späth, C. Donau, A. M. Bergmann, M. Kränzlein, C. V. Synatschke, B. Rieger and J. Boekhoven, *J. Am. Chem. Soc.*, 2021, **143**, 4782; (*e*) J. Heckel, S. Loescher, R. T. Mathers and A. Walther, *Angew. Chem., Int. Ed.*, 2021, **60**, 7717; (*f*) W. Zeng, C. Fan, X. Xing, H. Cheng, H. Fu, B. Ma, Z. Yang, R. Zhang and W. Zhang, *Giant*, 2021, **7**, 100067; (*g*) H. Xu, S. Bai, G. Gu, Y. Gao, X. Sun, X. Guo, F. Xuan and Y. Wang, *ACS Appl. Mater. Interfaces*, 2022, **14**, 43825.

5 (*a*) T. Fukui, S. Kawai, S. Fujinuma, Y. Matsushita, T. Yasuda, T. Sakurai, S. Seki, M. Takeuchi and K. Sugiyasu, *Nat. Chem.*, 2017, **9**, 493; (*b*) W. Qian, A. González-Campo, A. Pérez-Rodríguez, S. Rodríguez-Hermida, I. Imaz, K. Wurst, D. Maspoch, E. Ruiz, C. Ocal, E. Barrena, D. B. Amabilino and N. Aliaga-Alcalde, *Chem.–Eur. J.*, 2018, **24**, 12950; (*c*) R. Cao, G. Wang, X. Ren, P. Duan, L. Wang, Y. Li, X. Chen, R. Zhu, Y. Jia and F. Bai, *Nano Lett.*, 2022, **22**, 157.

6 (*a*) S. Okada and H. Segawa, *J. Am. Chem. Soc.*, 2003, **125**, 2792; (*b*) A. Satake and Y. Kobuke, *Org. Biomol. Chem.*, 2007, **5**, 1679; (*c*) S. Ogi, K. Sugiyasu, S. Manna, S. Samitsu and M. Takeuchi,

*Nat. Chem.*, 2014, **6**, 188; (*d*) N. J. Hestand and F. C. Spano, *Chem. Rev.*, 2018, **118**, 7069; (*e*) J. Singh, Theory of Excitons, in *Excitation Energy Transfer Processes in Condensed Matter. Physics of Solids and Liquids*, Springer, Boston, MA 1994, DOI: 10.1007/978-1-4899-0996-1_1.

7 (*a*) N. Nakajima and Y. Ikada, *Bioconjugate Chem.*, 1995, **6**, 123; (*b*) K. A. Totaro, X. Liao, K. Bhattacharya, J. I. Finneman, J. B. Sperry, M. A. Massa, J. Thorn, S. V. Ho and B. L. Pentelute, *Bioconjugate Chem.*, 2016, **27**, 994; (*c*) M. Tena-Solsona, C. Wanzke, B. Riess, A. R. Bausch and J. Boekhoven, *Nat. Commun.*, 2018, **9**, 2044.

8 (*a*) L. R. Knöpke, N. Nemati, A. Köckritz, A. Brückner and U. Bentrup, *ChemCatChem*, 2010, **2**, 273; (*b*) L. R. Knöpke, A. Spannenberg, A. Brückner and U. Bentrup, *Spectrochim. Acta, Part A*, 2012, **95**, 18.